

Evolution of a model dune in a shear flow

Kouamé Kan Jacques Kouakou^{a,b}, Pierre-Yves Lagrée^{b,*}

^a *Laboratoire de Mécanique Université de Cocody, Abidjan, Côte d'Ivoire*

^b *Laboratoire de Modélisation en Mécanique, U.M.R. CNRS 7607, Université Pierre et Marie Curie, boîte 162, 4, place Jussieu, 75252 Paris, France*

Received 13 December 2004; received in revised form 11 July 2005; accepted 19 September 2005

Available online 24 October 2005

Abstract

We present a simplified model for the displacement of a model dune in a constant viscous shear flow over a non-erodible soil. A simplified linear law with a threshold effect (in shear stress) and saturation is used to link the flux of sediments to the shear stress. The asymptotic framework of “Double Deck” (large Reynolds number laminar flow theory) is used for the flow. This method allows the computation of boundary layer separation, and the flow may be further simplified with an analytical relation linking the dune shape to the skin friction. For a given shape, the asymptotic solutions give a good agreement with Navier Stokes computations. Examples of displacement of model dunes are presented. We then obtain a selfsimilar coupled problem, predicting that the velocity of the dune is proportional to $m^{-1/4}$. Computations indicate that there is no dune if the mass of the dune is too small, or if the saturation length is too large, or if the threshold is too small.

© 2005 Elsevier SAS. All rights reserved.

Keywords: Boundary layer; Erosion sedimentation

1. Introduction

The study of ripples and dunes formation is attractive and receives a growing interest. It is a difficult problem to predict how a sand dune will emerge from the shore and move on the land, because one has to solve numerically the 3D turbulent Navier–Stokes equations for the air, where the viscosity is changed by the transported sand. Then the transport of sand in this flow has to be solved. Finally, the dune moves due to deposition and erosion and eventually avalanches may appear All those phenomena are strongly coupled, so that it is now nearly impossible to perform such computations. First for time consuming reasons, and second, for lack of exact physical knowledge of all the phenomena involved. Of course, the same difficulties arise when we deal with submarine dunes where air is replaced with water.

Sauermann et al. [1], Kroy et al. [2], and Andreotti et al. [3] solved a simplified but realistic coupled model for the displacement of aeolian dunes. Here, on one hand, we present some severe simplifications compared to their work, which allow us to obtain a simplified model problem that we go on to solve numerically. We put neither gravity effect nor avalanche effect. But, on the other hand, the key point in our model is that we make no approximation with

* Corresponding author.

E-mail address: pyl@ccr.jussieu.fr (P.-Y. Lagrée).

respect to the re-circulation bubble (they oversimplified the separation bulb). This is possible because the asymptotic framework we used allows boundary layer separation. Of course what we then call a “dune” or a model dune, is only the result of our simplified mathematical model and is quite far from reality. To a certain extent, it may be a first step in the direction of the study of small centimetric dunes in water such as Hersen et al. [4].

In Section 2.1, we recall the most simple way to obtain the flux of materials over an erodible soil, hence linking the saturated flux of materials (sand, sediments, etc.) to the shear stress τ . Two ingredients are retained namely, the existence of a threshold under which no sediments are moved, and a saturation length for the flux before it attains a saturated value. In Section 2.2, we assume that the basic flow is laminar and steady; namely, we assume that it is a simple shear flow (the velocity increases linearly with altitude). We assume that the dune is small in height so that its slope is small (compared to one). This approximation allows us to derive asymptotic solutions of the Navier–Stokes equations in the limit of large Reynolds numbers ($Re = \infty$). This is the so-called Triple Deck theory, see Stewartson and Williams [5], Neiland [6] (more precisely the Double Deck theory: Smith [7]). We note that Fowler [8] obtained a very similar description in over-simplifying a turbulent boundary layer. We compute the flow over a given bump with a Navier Stokes solver (CASTEM), and good agreement is found with the Double Deck computations. Then we present the coupled problem in Section 3, and solve it in Section 4. Following some examples of resolutions leading to the displacement at constant velocity of a “dune” in our simplified framework (either with non-linear or linear fluid solution), we propose a similar system of equations depending only on two final parameters. These parameters are the threshold value of the skin friction and a combination of the saturation length and the mass. Again, we find that there is a critical size under which no “dune” exist and that the larger the “dune” is, the slower it moves.

2. Basic equations

2.1. The erodible bed: relations between q and the flow

Du Boys [9] was one of the first to work on and to present a review of the subject. He understood that a critical value of the flow velocity must be reached in order to create a saturated flux of materials q_s . Since then (see Yang [10] who presents the other pioneering works such as: Exner (1925), Shields (1936), and Bagnold (1941), etc., as well as a comprehensive modern review), many other laws have been proposed, for which in general, the saturated flux of materials transported by the flow per unit width is an increasing function of the skin friction (or equivalently the shear stress: τ):

$$q_s = E\tau^a \varpi(\tau - \tau_s)^b, \quad (1)$$

where the threshold function ϖ is such that if $(\tau - \tau_s) > 0$, then $\varpi(\tau - \tau_s) = (\tau - \tau_s)$ else, $\varpi(\tau - \tau_s) = 0$. The coefficients a , b , E and τ_s depend on the modelling. The latter, when adimensionalised, is known as the threshold Shield number $\theta_s = \tau_s/(\rho_p - \rho)gd$; ρ and ρ_p are fluid and particle density, respectively, d is average particle diameter, and g is gravity. Flux arises when shear stress is high enough.

Du Boys [9] pioneering theoretical law corresponds to $a = b = 1$; Charru and Mouilleron-Arnould [11] used a law issued from (laminar) resuspension theory corresponding to $a = 0$, $b = 3$; Charru, Mouilleron-Arnould and Eiff [12] from laminar experiments in a annular channel, obtained $a = 1$, $b = 1$; in a turbulent water flow Sumer and Bakioglu [13] use $a = 1/2$, $b = 1$, Peter–Meyer (see Fredsøe and Deigaard [14]) use $a = 0$, $b = 3/2$; in a laminar water flow Blondeaux [15] uses $a = 0$, $b = 4.28$, in an eolian context Kroy et al. [2] use $a = 3/2$, $b = 0$. Those are the typical values.

The global scaling of the flux is a length time a velocity. In order to analyse experiments, the length used is mainly the grain diameter itself d . The velocity is mainly taken to be the settling velocity $((\rho_p - \rho)gd^2/\mu$ in laminar flows, $\sqrt{(\rho_p - \rho)gd}$ in turbulent flows). For instance, laminar experiments of [12] give:

$$q_s = 0.85 \frac{(\rho_p - \rho)gd^2}{18\mu} \left(\frac{\tau}{(\rho_p - \rho)gd} \right) \varpi \left(\frac{\tau}{(\rho_p - \rho)gd} - 0.12 \right), \quad (2)$$

whereas the usual Peter–Meyer law [14] for turbulent flows reads:

$$q_s = 8\sqrt{(\rho_p - \rho)gd^3} \varpi \left(\frac{\tau}{(\rho_p - \rho)gd} - 0.047 \right)^{3/2}. \quad (3)$$

Again, du Boys [9] observed among the firsts that this saturated flux is not abruptly obtained when the flow goes from a non-erodible part of the bed to an erodible one. There is a settling distance. Sauermann et al. [1], Kroy et al. [2] obtained this in solving a simplified equation for the saltating grains of sand in air. Andreotti et al. [3] simplified it and reformulated this phenomena of saturation as:

$$l_s \frac{\partial}{\partial x} q + q = q_s, \quad (4)$$

where l_s is the settling or saturation length. This relation represents the relaxation of the value of the flux toward the final admissible saturated value. This length is estimated to be of order $\rho_p/\rho d$ in water Charru and Hinch [16] or in air [3]. Eq. (4) may be viewed as a conservation of the mass of sediments in the flow (Charru and Hinch [16] or Lagrée [17] or Valance and Langlois [18]) when supposing that the time variation of the soil is slower than the flow time scale. With this point of view q/l_s

and the matching with the shear flow either far from the soil ($\bar{y} \rightarrow \infty$) or far upstream ($\bar{x} \rightarrow -\infty$):

$$\lim_{\bar{y} \rightarrow \infty} \bar{u}(\bar{x}, \bar{y}) = \lim_{\bar{x} \rightarrow -\infty} \bar{u}(\bar{x}, \bar{y}) = \bar{y}, \quad \lim_{\bar{x} \rightarrow -\infty} \bar{v}(\bar{x}, \bar{y}) = 0. \tag{10}$$

This system contains non-linear inertial effects, and viscous effects (it is the Boundary Layer equations system with different scales and boundary conditions). It is known to allow to compute boundary layer separation (Sychev et al. [22]).

As the basic flow $\bar{u} = \bar{y}, \bar{v} = 0, \bar{p} = 0$, is a solution of the system (8)–(10), there is a classical analytical solution for the linearized equations. It is supposed that the slope of the wall is weak in order to allow this linearization. Looking at solutions in Fourier space, we find the expression of the skin friction at the wall as:

$$\bar{\tau} = 1 + (TF^{-1}[(3Ai(0))(-i\bar{k})^{1/3}TF[\bar{f}]]) + \dots, \tag{11}$$

where TF denotes the Fourier transform and Ai is the Airy function.

To settle those equations, we insist on the fact that we have supposed that the sediments do not change the flow. The viscosity remains the same, and the boundary condition on the interface, which is supposed well-defined, is always a no-slip condition. We have also supposed that the time of displacement of the model dune is so slow that a quasi steady solution for the fluid is pertinent.

2.2.2. Comparing solutions for a given fixed soil

Having a given fixed topography $\bar{f}(\bar{x})$ we are able to compute the steady flow. First, we solve the full Navier–Stokes (using the code CASTEM 2000 [23]). Second, using a finite difference scheme, we solve the “Inverse Boundary Layer” system (8)–(10), with the FLARE approximation (Cebeci and Cousteix [24]). Third, using Fast Fourier Transform algorithms (Press et al. [25], and Ooura [26]) we solve (11). We compare the three approaches (at $Re = 1000$ for CASTEM, on Figs. 1 and 2) for a bump in Double Deck scales: $\bar{y} = \bar{f}(\bar{x})$ with $\bar{f}(\bar{x}) = \alpha \exp(-\bar{x}^2)$. We see that the Double Deck under predicts the skin friction maximum. The longitudinal scale λ for the full Navier Stokes is the same as the Double Deck scale. So, if h_0 is the height of the bump, $h_0/\lambda = \alpha Re^{-1/3}$ (the aspect ratio is of order $Re^{-1/3} = 0.1$, this kind of value is the order of magnitude of slopes in ripples or dunes). On Fig. 1 we have $\alpha = 1$ and $h_0/\lambda = 0.1$; on Fig. 2, $\alpha = 2$ and $h_0/\lambda = 0.2$. We see that for small α , the three computations are nearly the same (if $\alpha < 1$ the three approaches are nearly equivalent, see Fig. 1). The influence of non-linearity appears for a reduced

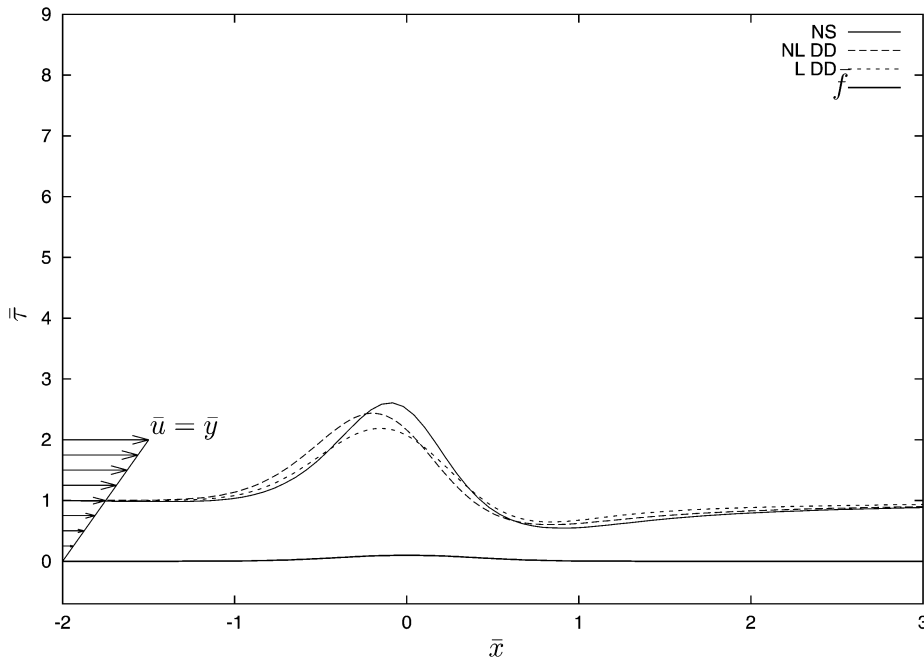


Fig. 1. Comparing shear stress for Navier–Stokes (NS), non-linear full Double Deck equations (NL DD), and linearized Double Deck equations (L DD), $\alpha = 1, Re = 1000$. The three descriptions are similar for $\alpha < 1.5$.

angle $\alpha > 1.5$. Incipient flow separation occurs at $\alpha \simeq 2.1$ for the non-linear Double Deck equations, while using the linearized solutions gives a value of $\alpha \simeq 3.3$. On Fig. 3 we plot this Double Deck asymptotic prediction ($\alpha \simeq 2.1$) and several full Navier Stokes computations. Changes in trend are due to changes in mesh which is more and more refined as Re increases and to the difficulty to find the incipient value. The Double Deck prediction of the height of

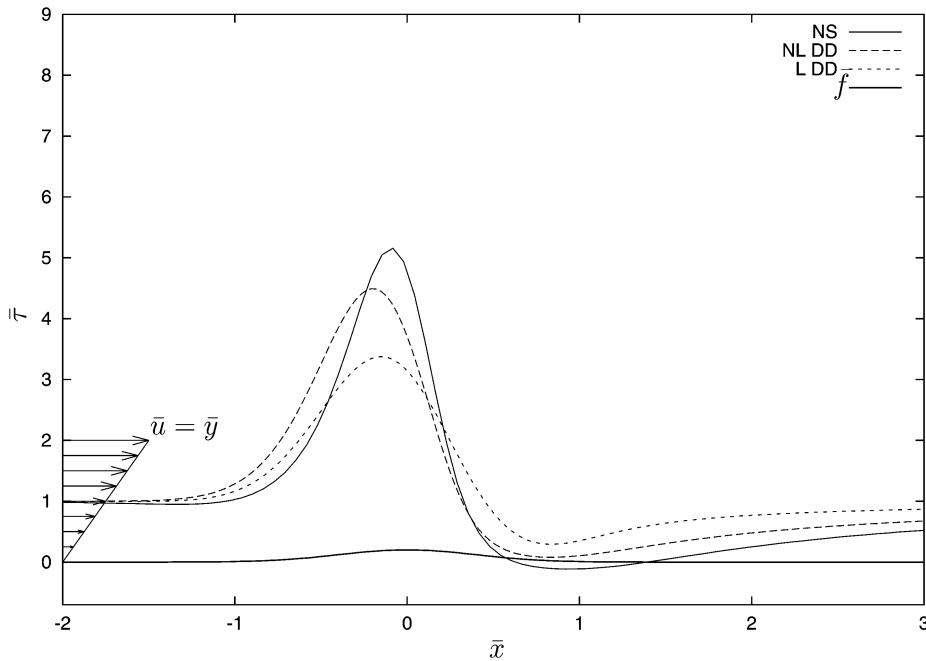


Fig. 2. Comparing Navier–Stokes (NS), non-linear full Double Deck equations (NL DD), and linearized Double Deck equations (L DD), $\alpha = 2$, $Re = 1000$.

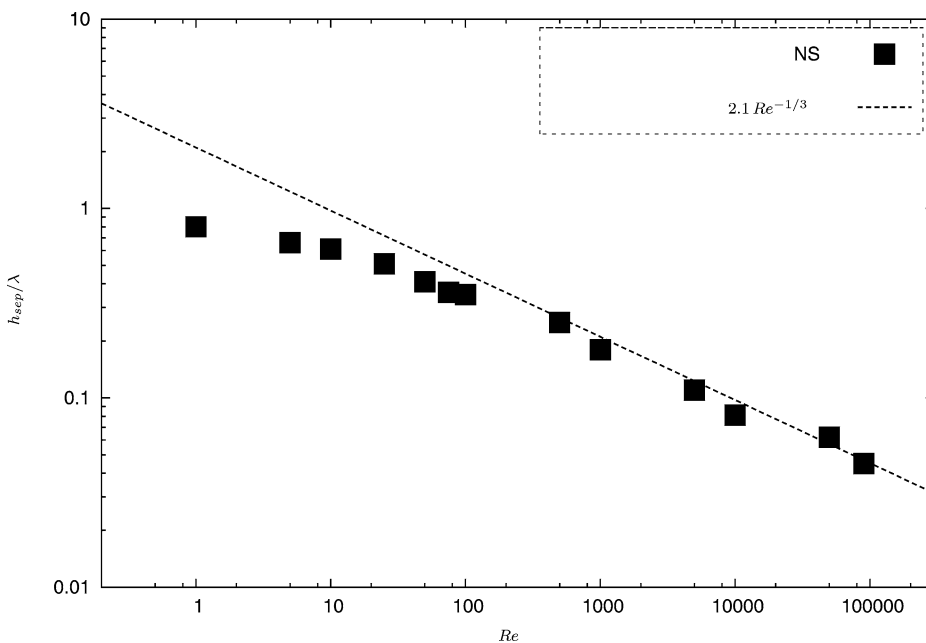


Fig. 3. Value of the relative height of the Gaussian bump at incipient separation. Comparing full numerical Navier–Stokes (squares) and the prediction from the non-linear Double Deck equations (line). The asymptotic theory well predicts the height of incipient separation.

separation is correct even for moderate values of Re , while the linearized Double Deck over predicts this value. This observation, and the paper by Bhattacharyya et al. [27], give us confidence in the linearized solution (11) for small bumps and show that even this simple linear solution gives a good enough prediction for flow separation. This means that at least the overall distribution of skin friction is good. Showing a strong increase of the skin friction before the crest, and a decrease of the skin friction which begins just before the crest. The increase of skin friction is responsible of the erosion of the bump, the decrease may lead to boundary layer separation. now formula 11 to compute the flow.

3. The adimensionalised coupled problem

Now, we have the no-dimensional equations for the flow. For the sediments, we will write $q = Q_0 \bar{q}$ where $Q_0 = E(\mu U_0')^{a+b}$, $\bar{\tau}_s = \theta_s(\rho_p - \rho)gd/(\mu U_0')$ and use as time scale $T = (v\phi^3\lambda^4/(U_0'Q_0^3))$. This time scale is supposed to be slow compared to the flow time scale. Therefore, the final model problem consists in solving, for an initial given topography $\bar{f}(\bar{x}, \bar{t} = 0)$, the flow (8)–(10) or the simplified formula (11) with mass conservation written without dimension, that is (6) (written with the scales of Subsection 2.2.1):

$$\frac{\partial \bar{f}}{\partial \bar{t}} + \frac{\partial \bar{q}}{\partial \bar{x}} = 0, \quad (12)$$

and the suitably adimensionalized version of (7) (with scales of Subsection 2.2.1):

$$\bar{l}_s \frac{\partial}{\partial \bar{x}} \bar{q} + \bar{q} = \varpi(\bar{\tau} - \bar{\tau}_s), \quad (13)$$

where \bar{l}_s , and $\bar{\tau}_s$ are without dimensions. We suppose that all the parameters are of order one in order to have the maximum of phenomena modeled in the equations.

If no special constrain is given on \bar{f} , this means that the soil is fully erodible. It has been shown in Lagrée [17] and in Kouakou and Lagrée [28] that this system is linearly unstable (when (11) is used to solve the flow). It has also been shown, that if this system is solved for large time, starting with a given initial random small topography, and with a cyclic boundary condition (FFT resolution), then as time increases ripples appear. Those ripples grow and coarsen: they merge. Finally, there is only one single bump in the computational box which moves at a constant velocity without changing shape.

4. Displacement of a model dune, linear and non-linear Double Deck

4.1. The dune over a non-erodible soil

In Kouakou and Lagrée [28], Eqs. (11), (12), and (13) are solved starting from any initial profile, in the case of fully erodible soil, leading eventually to a single bump in the computational box. It does not “dig” under a final depth, and it seems to stay as it moves over an non-erodible soil. However, this is not equivalent to solve the movement of a single “dune” on a real non-erodible flat soil. Because the cyclic boundary condition perturbrates the bump itself. This perturbation is due to the skin friction slowly going back to its non-perturbed value.

In order to solve the displacement of an initial model dune of erodible material with given “mass” (represented by $\bar{m} = \int_{-\infty}^{\infty} \bar{f}(\bar{x}, \bar{t} = 0) d\bar{x}$) over a non-erodible flat soil, we have to exclude erosion under the flat soil $\bar{y} = 0$, so that $\bar{f}(\bar{x}, \bar{t})$ must always be positive. So, we have to be careful with the term $\bar{q}_s = \varpi(\bar{\tau} - \bar{\tau}_s)$ in order to avoid “digging” under $\bar{y} = 0$. In fact, as the scheme is explicit in time, at each position \bar{x} , we compute the value of \bar{q}_s (say $\bar{q}_{s \max}$) which gives $\bar{f}(\bar{x}, \bar{t} + \Delta \bar{t}) = 0$. If $\bar{q}_s = \varpi(\bar{\tau} - \bar{\tau}_s) < \bar{q}_{s \max}$, the elevation is positive $\bar{f}(\bar{x}, \bar{t} + \Delta \bar{t}) > 0$, which is fine. If $\bar{q}_s > \bar{q}_{s \max}$, then $\bar{f}(\bar{x}, \bar{t} + \Delta \bar{t}) < 0$, which is excluded, and in this case we put $\bar{q}_s = \bar{q}_{s \max}$ so that $\bar{f}(\bar{x}, \bar{t} + \Delta \bar{t}) = 0$. Physically, this means that we do not dig into the non-erodible wall. Eventually, the domain must be large enough in order to prevent lee effects to influence the stoss side. We obtain the long time shape (\bar{f}_{fin}) of the dune and its velocity (\bar{c}), so that $\bar{f}(\bar{x}, \bar{t} \gg 1) = \bar{f}_{\text{fin}}(\bar{x} - \bar{c}\bar{t})$ and finally $\bar{q}_{\text{fin}} = \bar{c} \bar{f}_{\text{fin}}(\bar{x} - \bar{c}\bar{t})$. So, for a given material ($\bar{\tau}_s$, and \bar{l}_s), with a given mass, we obtain the velocity $\bar{c}(\bar{\tau}_s, \bar{l}_s, \bar{m})$ as an eigenvalue.

4.2. Example of time evolution: linear and non-linear Double Deck

For the initial bump, whether we choose either an arch of sine function or a Gaussian function for instance is irrelevant because only the value of the “mass”, defined as the integral of the function, is the pertinent parameter. As an illustrative example of the resolution of (8)–(10) and (12)–(13), we plot on Fig. 4 top and middle two examples with same mass, but with different initial shape (with two different aspect ratio). The initial shape does not matter. The final shape is the same, the mass has not changed, but the history is different: one increases in height and decreases in length, the other does the opposite. Fig. 4 bottom shows a case where no dune persists: if the mass is too small, the dune is washed and disappears.

In order to avoid that the “dune” goes out the domain, we add the term $-\bar{c} \frac{\partial \bar{f}}{\partial \bar{x}}$ to the right-hand side of (12) to move with the “dune”. The value of the celerity c is obtained from the value of the flux and the value of the bump at its crest: $\bar{c} = \bar{q}(\bar{x}_{\max})/\bar{f}_{\max}$. The solution is now plotted in the moving frame so that every curve is centered in 0. After a while we obtain the final steady shape \bar{f}_{fin} . For example we first show a linear (11) example, we plot on Fig. 5 top the final linearly solved bump obtained in a case where mass is conserved. The skin friction and the associated saturated flux are plotted, the actual flux \bar{q} is plotted too. A steady solution is obtained in the moving frame. We plot on Fig. 5 bottom a linearly solved bump (at time $\bar{t} = 1$), in this case the mass is too small, the dune losses mass. There is no steady solution. The flux of mass is not zero at the end of the model dune.

We plot on Fig. 6 the final bump obtained for various masses. The linear resolution and the non-linear resolution are plotted, i.e. we compare solution of (11) to the solution of (8)–(10) for the flow. We observe that the non-linearity flattens the stoss side, while the lee-side remains nearly the same. The velocity of the dune is larger in the non-linear case than in the linear case. The effect of non-linearity is the effective computation of the boundary layer separation. This separation occurs here for $\bar{m} > 4.9$ (when $\bar{\tau}_s = 0.9$, $1/\bar{l}_s = 2.5$). We plot on Fig. 7 an example of non-linear computation of a dune with $\bar{m} = 6$ with boundary layer separation: we find that there is a separation bubble in the lee side ($\bar{\tau} < 0$). The same case, but linear, is displayed as well. The size of the separation bulb is under predicted by the linearized formula.

It is then observed that possible model dunes are of rather large mass and of length larger than one. So we will try in the next section to fix the mass of the dune and find a self-similarity in the equations.

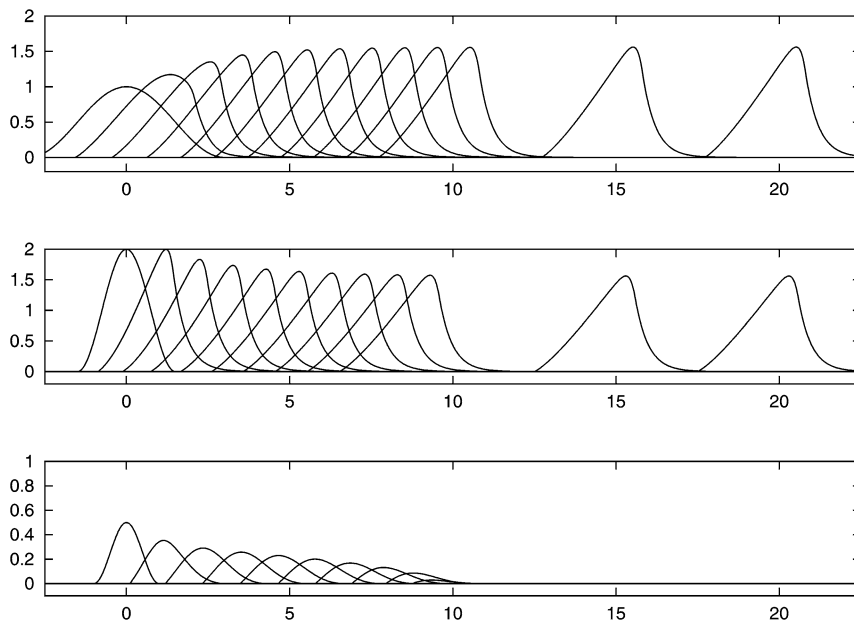


Fig. 4. The non-linear Double Deck evolution of three “dunes”, for $\bar{t} = 0, 1, 2, \dots, 10, \bar{t} = 15$, and $\bar{t} = 20$. Two upper curves: $\bar{m} = 3$ is conserved, $\bar{\tau}_s = 0.9$, and $1/\bar{l}_s = 2.5$, but two different initial shapes leading to the same final solution. Lower curve: $\bar{m} = 0.5$; when the initial mass is too small, the “dune” is washed, it loses mass.

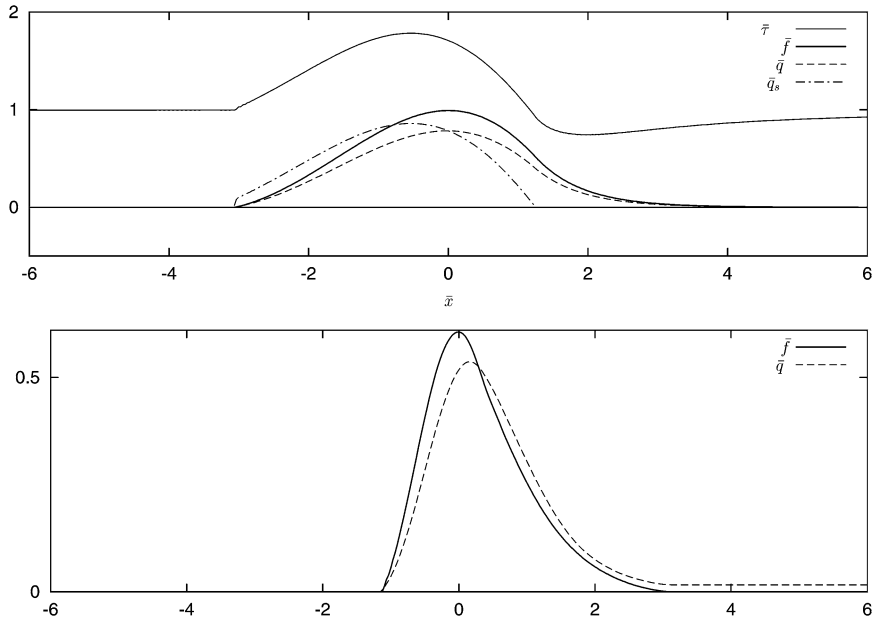


Fig. 5. Two linear Double Deck examples of model dune in the moving frame, $\bar{\tau}_s = 0.9$, and $1/\bar{l}_s = 1.5$. On the upper curve $\bar{m} = 3$ is conserved, plot of the skin friction, associated saturated flux and value of the actual flux. On the lower curve, $\bar{m} = 1$, plot of the skin friction, and value of the flux \bar{q} . The non-zero value of \bar{q} after the end of the model dune shows that there is loss of mass.

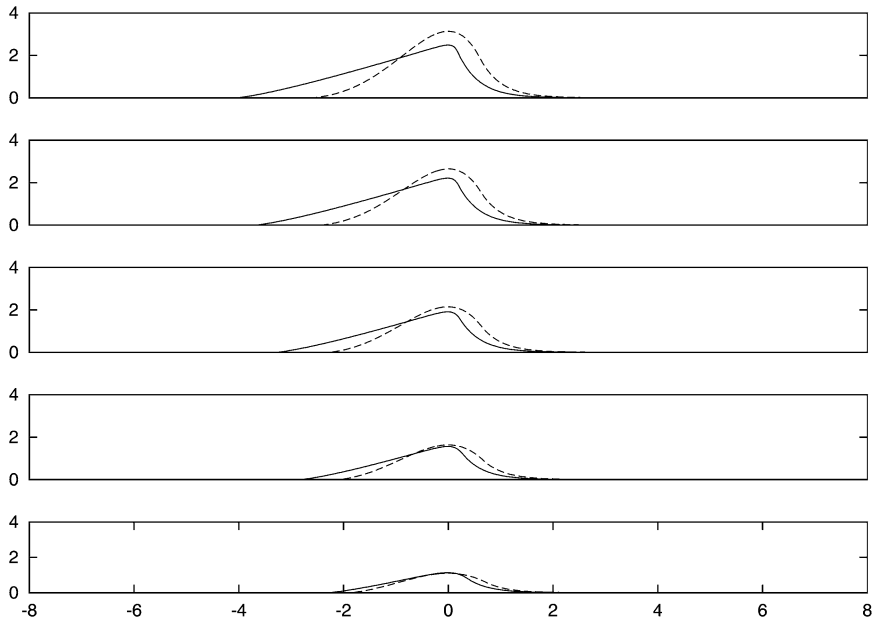


Fig. 6. The non-linear final moving “dune” solution $\bar{f}_{fin}(\bar{x} - \bar{c}\bar{t})$ is represented with solid lines, the linear solution is represented with dashed lines, and $\bar{\tau}_s = 0.9$, $1/\bar{l}_s = 2.5$, $\bar{m} = 2, 3, 4, 5, 6$ (bottom curve to top curve).

4.3. Self similarity: linearized Double Deck

Given any positive values L , F , T , and Q , we rescale the variables through: $\bar{x} = Lx^*$, $\bar{f} = Ff^*$, $\bar{\tau} = \Gamma\tau^*$, $\bar{t} = Tt^*$, and $\bar{q} = Qq^*$. It is then possible to obtain a selfsimilar solution of the system (11), (12), and (13). This complexity of

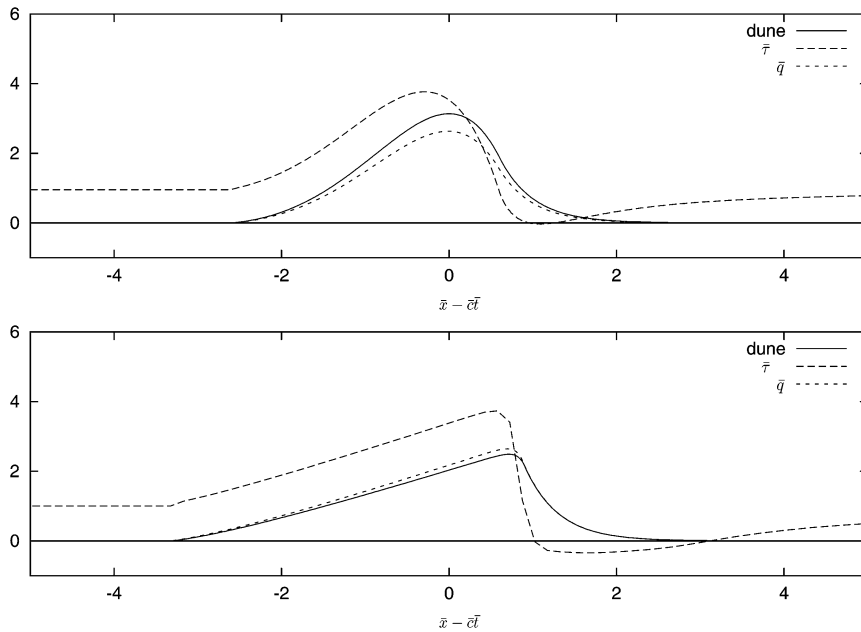


Fig. 7. An example of a final moving “dune” solution ($\bar{\tau}_s = 0.9, 1/\bar{l}_s = 2.5, \bar{m} = 6$). Upper curve, the linear case. The extrapolated skin friction is slightly negative. Lower curve, the non-linear case: the stoss side is nearly flat. The skin friction is represented; it is negative in the lee side: there is boundary layer separation.

the exploration of the parameters is then reduced. We have $F = L^{1/3}$ so that the skin friction is invariant (due to the fact that the threshold is given):

$$\bar{\tau} = 1 + L^{-1/3} L^{1/3} TF^{-1}[(3Ai(0))(-ik^*)^{1/3} TF[f^*]] = \tau^*.$$

Upon inspection, the final rescaling: $\bar{x} = \bar{m}^{3/4} x^*, \bar{f} = \bar{m}^{1/4} f^*, \bar{\tau} = \tau^*, \bar{t} = \bar{m} t^*,$ and $\bar{q} = q^*$ gives the final unit mass selfsimilar problem:

$$(l_s^*) \frac{\partial q^*}{\partial x^*} + q^* = \varpi (\tau^* - \tau_s^*),$$

$$\frac{\partial f^*}{\partial t^*} = -\frac{\partial q^*}{\partial x^*}, \quad \int f^* dx^* = 1.$$

Hence the sole parameters are: $(l_s^*)^{-1} = (\bar{l}_s^{-1} \bar{m}^{3/4})$ and: τ_s^* (which is exactly $\bar{\tau}_s$). The result is the final bump shape and its velocity c^* , which is such that $c^* f^* = q^*$.

On Fig. 8 we plotted the velocities of the “dunes” c^* for several values of l_s^* and τ_s^* . We find that the “dunes” do not always exist: if l_s^* is too large (depending on the threshold value), there is no steady solution. For example, if $(\bar{l}_s^*)^{-1} < 3.8$ for $\tau_s^* = 0.9$ (or if $(l_s^*)^{-1} < 4.9$ for $\tau_s^* = 0.8$) there is no steady solution of constant mass, and the initial given dune loses materials and disappears. If the threshold is decreased, then the minimal mass is increased. On Fig. 9 we plot the final unit mass model dune for several values of l_s^* (those curves are the rescaled dunes for non-unit mass cases too). We see that the smaller l_s^* is, the higher and thinner the bump is. It does not seem possible to have a “dune” with $l_s^* = 0$, i.e. with $q^* = \tau^*$.

So, at fixed $\bar{\tau}_s$, for a given mass \bar{m} , and a given saturation length \bar{l}_s , the curve of Fig. 8 gives:

$$\frac{1}{\bar{c}} = \bar{m}^{1/4} c^* ((\bar{l}_s^{-1} \bar{m}^{3/4}), \bar{\tau}_s). \tag{14}$$

It is interesting to note that this model is different from the model proposed by Andreotti et al. [3], where the skin friction involves the Hilbert integral corresponding to the inviscid perturbation of the flow $\int_{-\infty}^{\infty} \frac{f'}{x-\xi} d\xi$. In this case the rescaling is $x = m^{1/2} x^*, f = m^{1/2} f^*, \tau = \tau^*, t = mt^*,$ and $q = q^*$. So that $1/c$ is proportional to $m^{1/2}$. This relation is well supported by real dunes. This dependence is then due to the specific skin friction expression (linked here to the inviscid perturbation of the flow).

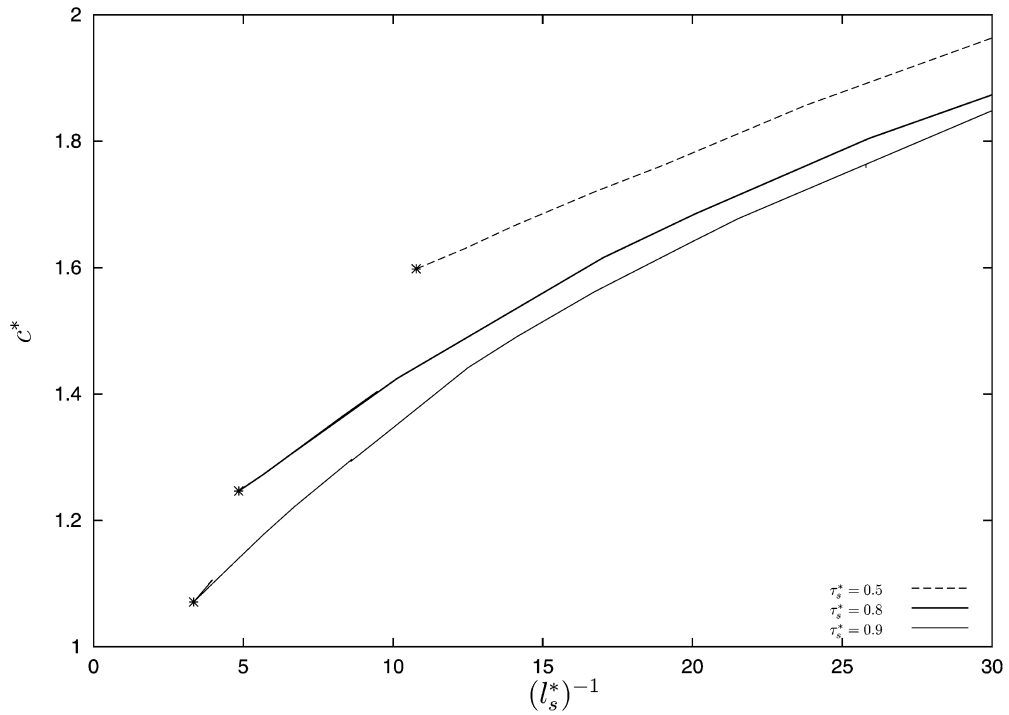


Fig. 8. The selfsimilar relation between the mass \bar{m} , the inverse of the saturation length $l_s^* = \bar{l}_s \bar{m}^{-3/4}$, and the velocity $c^* = \bar{c} \bar{m}^{1/4}$ of the “dune” for three values of the threshold: $\tau_s^* = 0.9, 0.8,$ and 0.5 . For a fixed threshold, there is a maximal value of the saturation length l_s^* over which there is no solution.

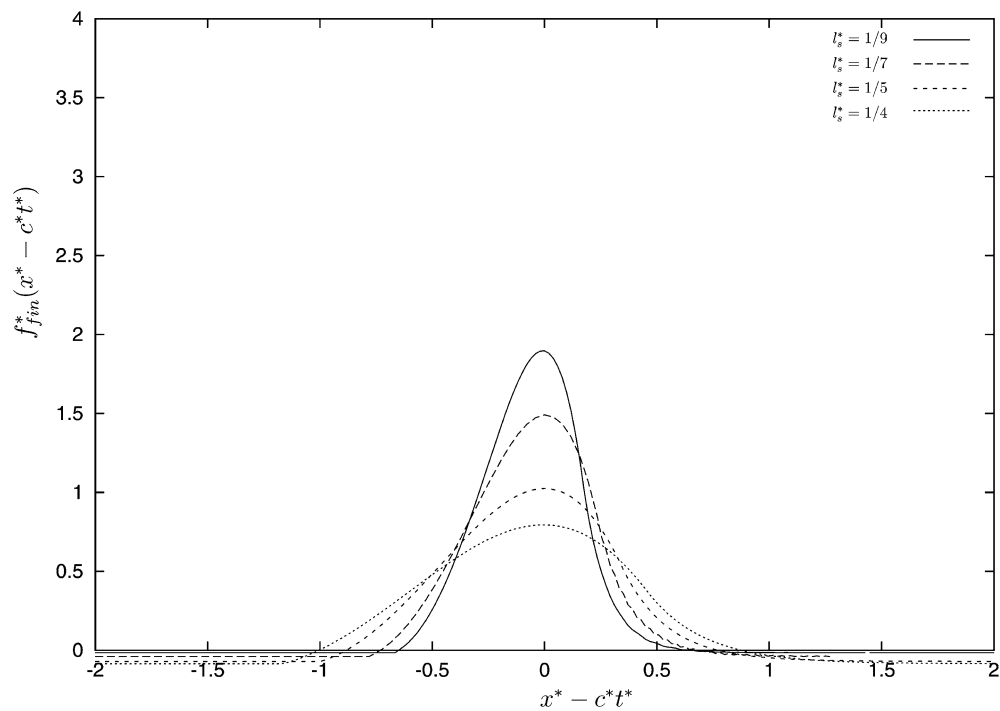


Fig. 9. “Dunes” of unit mass with $l_s^* = 1/4, 1/5, 1/7, 1/9$ ($\tau_s^* = 0.9$). The smaller l_s^* is, the thinner and higher the “dune” is. For $l_s^* = 0$ (i.e. $q^* = \tau^*$), there is no dune.

5. Further possible developments

A first possibility would be to explore another classical case of the $\bar{q}(\bar{\tau})$ relation. A slope correction for the threshold value (Bagnold [29]) may be introduced to take into account the fact that it is more difficult to move the sediments uphill than downhill. The adimensionalized flux is then supposed to be always saturated:

$$\bar{q} = \varpi \left(\bar{\tau} - \bar{\tau}_s - \bar{\Lambda} \frac{\partial \bar{f}}{\partial \bar{x}} \right), \tag{15}$$

where we may estimate the gravity effect as $\bar{\Lambda} = \theta_s (\rho_p - \rho) g d Re^{-1/3} / \tan(\phi_d)$, with $\tan(\phi_d)$ the static friction angle. The system (11), (12), and (15) also admits a selfsimilar solution. This property introduces $\bar{\Lambda} \bar{m}^{-1/2}$ as sole parameter in (15): $q^* = \varpi (\tau^* - \tau_s^* - \bar{\Lambda} \bar{m}^{-1/2} \partial f^* / \partial x^*)$. We would then obtain the velocity of the “dunes” as:

$$\frac{1}{\bar{c}} = \bar{m}^{1/4} c^* ((\bar{\Lambda} \bar{m}^{-1/2}), \bar{\tau}_s). \tag{16}$$

An other possibility is to construct the 3D counterpart of this problem. After some algebra (in the spirit of Smith and Gajjar [30]), the skin friction in the Fourier space is found to be given by:

$$\begin{aligned} \bar{\tau}_x &= 1 + TF^{-1} [3(-i\bar{k}_x)^{1/3} Ai(0) a(\bar{k}_x, \bar{k}_z) TF[\bar{f}]], \\ \bar{\tau}_z &= TF^{-1} \left[3((-i\bar{k}_x)^{1/3} Ai(0)) \frac{\bar{k}_x b(\bar{k}_x, \bar{k}_z)}{\bar{k}_z} TF[\bar{f}] \right], \\ b(\bar{k}_x, \bar{k}_z) &= \frac{(-3Ai'(0))\bar{k}_z^2}{9Ai(0)^2(\bar{k}_x^2 + \bar{k}_z^2)}, \quad a = (1 - b(\bar{k}_x, \bar{k}_z)). \end{aligned}$$

The problem is then to extend to 3D flows the flux/shear relation, this has been proposed by Hersen et al. [4] and [31].

Finally, we think that a more realistic way to explore is to solve the turbulent counterpart of our problem. This is the case of a dune in a thick turbulent boundary layer. In that case, a mixing length must be introduced in the diffusive term in (8), so that $\frac{\partial^2}{\partial y^2} \bar{u}$ is changed in its counterpart

$$\frac{\partial}{\partial y} \left\{ \left(\nu + \ell^2 \left\| \frac{\partial u}{\partial y} \right\| \right) \frac{\partial u}{\partial y} \right\}$$

(written with dimensions). Here ℓ is for example the Cebeci Smith algebraic viscosity (Cebeci and Cousteix [24]). The boundary condition upstream is found through the matching with a logarithmic boundary layer.

If needed, we may introduce an avalanche effect, preventing the slope of the “dune” to become larger than the avalanche angle.

6. Conclusion

We proposed a simplified model for the movement of a dune over a rigid soil in a pure shear flow. The flow is supposed steady and bidimensional. Perturbations remain confined in a viscous layer near the soil. Comparisons between the linearized asymptotic solution, the full asymptotic relation, and a full Navier–Stokes resolution were drawn in order to justify the flow simplifications. We presented examples of displacements of dunes with linearized asymptotic solution, and the full asymptotic relation. We computed the boundary layer separated bubble.

We also obtained a self-similar problem, predicting that the velocity of the model dune scales with the inverse the power 1/4 of the mass, while the function in the prefactor is itself a function of the mass. We observed that if the dune is too small, then it disappears; that at fixed mass, an increase in the saturation length gives the same result; and finally, that at constant mass and constant saturation length, a decrease in the threshold value has the same consequence.

These results are for our “model dune” which is a bit unrealistic. It is nevertheless a first step to explain small water dunes in experimental setups. A lot of things will change for real dunes, nevertheless, the global method and some conclusions will be the same. For model and real dune, there exists a minimal dune size and a special selfsimilarity. To be more realistic, first, one has to introduce turbulence as suggested, and a ideal fluid layer, this will allow to recover the velocity in the inverse square root of the mass. It is likely that for both real and model dune the flattening of the stoss side is due to non-linear convective effects. Finally, we computed cases with flow separation and compared linearized and non-linearized cases which was not done before.

References

- [1] G. Sauermaun, K. Kroy, H.J. Herrmann, A continuum saltation model for sand dunes, *Phys. Rev. E* 64 (3 Pt 1) (2001) 031305.
- [2] K. Kroy, G. Sauermaun, H.J. Herrmann, A minimal model for sand dunes, *Phys. Rev. Lett.* (2002) 054301.
- [3] B. Andreotti, P. Claudin, S. Douady, Selection of dune shapes and velocities. Part 2: A two-dimensional modelling, *Eur. Phys. J. B* 28 (2002) 341–352.
- [4] P. Hersen, S. Douady, B. Andreotti, Relevant length scale of barchan dunes, *Phys. Rev. Lett.* 89 (26) (2002) 264301.
- [5] K. Stewartson, P.G. Williams, Self-induced separation, *Proc. Roy. Soc. Ser. A* 312 (1969) 181–206.
- [6] V.Ya. Neiland, Propagation of perturbation upstream with interaction between a hypersonic flow and a boundary layer, *Mekh. Zhidk. Gaza* 4 (1969) 53–57.
- [7] F.T. Smith, Flow through constricted or dilated pipes and channels, parts 1 and 2, *Q. J. Mech. Appl. Math.* 29 (1976) 343–364.
- [8] A.C. Fowler, Dunes and Drumlins, in: N.J. Balmforth, A. Provenzale (Eds.), *Geomorphological Fluid Mechanics*, in: *Lecture Notes in Phys.*, vol. 582, Springer, 2001, pp. 430–454.
- [9] P. du Boys, Le Rhône et les rivières à lit affouillable, *J. Ann. Ponts et Chaussées, Sér. 5* 18 (1879) 141–195;
P. du Boys, Etude du régime et de l'action exercée par les eaux sur un lit à fond de graviers indéfiniment affouillable (Study of flow regime and force exerted on a gravel bed of infinite depth), *Ann. Ponts et Chaussées, Paris, France, Sér. 5* 19 (1879) 141–195.
- [10] C.T. Yang, *Sediment Transport: Theory & Practice*, McGraw-Hill Education Europe, 1995, 480 p.
- [11] F. Charru, H. Mouilleron-Arnould, Instability of a bed of particules sheared by a viscous flow, *J. Fluid Mech.* 452 (2002) 303–323.
- [12] F. Charru, H. Mouilleron-Arnould, O. Eiff, Erosion and deposition of particles on a bed sheared by a viscous flow, *J. Fluid Mech.* 519 (2004) 55–80.
- [13] B.M. Sumer, M. Bakiogoglu, Formation of ripples on an erodible bed, *J. Fluid Mech.* 144 (1984) 177–190.
- [14] J. Fredsøe, R. Deigaard, *Mechanical of Coastal Sediment Transport*, *Advanced Series on Ocean Engineering*, vol. 3, World Scientific, 1992, 392 p.
- [15] P. Blondeaux, Sand ripples under sea waves. Part 1. Ripple formation, *J. Fluid Mech.* 218 (1990) 1–17.
- [16] F. Charru, E.J. Hinch, Ripple formation on a particule bed sheared by a viscous liquid. Part one: steady flow, submitted for publication.
- [17] P.-Y. Lagrée, A Triple Deck model of ripple formation and evolution, *Phys. Fluids* 15 (8) (2003) 2355–2368.
- [18] A. Valance, V. Langlois, Ripples formation of over a sand bed submitted to a laminar shear flow, *Eur. Phys. J. B* 43 (2005) 283–294.
- [19] F.T. Smith, P.W.M. Brighton, P.S. Jackson, J.C.R. Hunt, On boundary-layer flow past two-dimensional obstacles, *J. Fluid Mech.* 113 (1981) 123–152.
- [20] S. Saintlos, J. Mauss, Asymptotic modelling for separating boundary layers in a channel, *Int. J. Engrg. Sc.* 34 (1996) 201–211.
- [21] L. Plantier, Le problème de la couche interne des écoulements asymptotiques de type triple couche: modèle, analyse et simulations, PhD thesis, Université Paul Sabatier, Toulouse, France, 1997.
- [22] V.V. Sychev, A.I. Ruban, V.V. Sychev, G.L. Korolev, *Asymptotic Theory of Separated Flows*, Cambridge University Press, 1998.
- [23] CEA-DEN/DM2S/SEMT, <http://www-cast3m.cea.fr>.
- [24] T. Cebeci, J. Cousteix, *Modeling and Computation of Boundary Layer Flows*, Springer-Verlag, 1999.
- [25] W.H. Press, B.P. Flannery, S.A. Teukolsky, W.T. Vetterling, *Numerical Recipes in C: The Art of Scientific Computing*, Cambridge University Press, 2002.
- [26] T. Ooura, <http://momonga.t.u-tokyo.ac.jp/~ooura/>.
- [27] S. Bhattacharyya, S.R.C. Dennis, F.T. Smith, Separating flow past a surface-mounted blunt obstacle, *J. Engrg. Math.* 3 (2001) 47–62.
- [28] K.K.J. Kouakou, P.-Y. Lagrée, Stability of an erodible bed in various shear flows, *Eur. Phys. J B* (2003), in press.
- [29] R.A. Bagnold, An approach to the sediment transport problem from general physics, in: *The Physics of Sediments and Transport by Wind and Water*, Amer. Society of Civil Engineers, 1988.
- [30] F.T. Smith, J. Gajjar, Flow past wing-body junctions, *J. Fluid Mech.* 144 (1984) 191–215.
- [31] P. Hersen, K.H. Andersen, H. Elbelrhiti, B. Andreotti, P. Claudin, S. Douady, Corridors of barchan dunes: stability and size selection, *Phys. Rev. E* 69 (2004) 011304.